IAI Journals.ASM.org

Outer Surface Protein OspC Is an Antiphagocytic Factor That Protects *Borrelia burgdorferi* from Phagocytosis by Macrophages

Sebastian E. Carrasco,[a] Bryan Troxell,[a]* Youyun Yang,[a] Stephanie L. Brandt,[a] Hongxia Li,[a] George E. Sandusky,[b] Keith W. Condon,[c] C. Henrique Serezani,[a] X. Frank Yang[a]

Department of Microbiology and Immunology, Indiana University School of Medicine, Indianapolis, Indiana, USA[a]; Department of Pathology and Laboratory Medicine, Indiana University School of Medicine, Indianapolis, Indiana, USA[b]; Department of Anatomy and Cell Biology, Indiana University School of Medicine, Indianapolis, Indiana, USA[c]

Outer surface protein C (OspC) is one of the major lipoproteins expressed on the surface of *Borrelia burgdorferi* during tick feeding and the early phase of mammalian infection. OspC is required for *B. burgdorferi* to establish infection in both immunocompetent and SCID mice and has been proposed to facilitate evasion of innate immune defenses. However, the exact biological function of OspC remains elusive. In this study, we showed that the *ospC*-deficient spirochete could not establish infection in NOD-*scid IL2rγ*^{null} mice that lack B cells, T cells, NK cells, and lytic complement. The *ospC* mutant also could not establish infection in anti-Ly6G-treated SCID and C3H/HeN mice (depletion of neutrophils). However, depletion of mononuclear phagocytes at the skin site of inoculation in SCID and C3H/HeN mice allowed the *ospC* mutant to establish infection *in vivo*. In phagocyte-depleted mice, the *ospC* mutant was able to colonize the joints and triggered neutrophilia during dissemination. Furthermore, we found that phagocytosis of green fluorescent protein (GFP)-expressing *ospC* mutant spirochetes by murine peritoneal macrophages and human THP-1 macrophage-like cells, but not in PMN-HL60, was significantly higher than parental wild-type *B. burgdorferi* strains, suggesting that OspC has an antiphagocytic property. In addition, overproduction of OspC in spirochetes also decreased the uptake of spirochetes by murine peritoneal macrophages. Together, our findings provide evidence that mononuclear phagocytes play a key role in clearance of the *ospC* mutant and that OspC promotes spirochetes' evasion of macrophages during early Lyme borreliosis.

Lyme disease, the most prevalent vector-borne illness in the United States (1), is a multisystem inflammatory disorder caused by infection with the spirochete *Borrelia burgdorferi* (2, 3). This spirochete is maintained in nature through a complex enzootic cycle involving *Ixodes* ticks and various small-mammal hosts. Humans, as accidental hosts, become infected after *B. burgdorferi*-infected ticks feed on them (4). Spirochetes replicate in the skin, spread locally, and induce an inflammatory response with a symptom known as erythema migrans, observed in most patients (2, 4). During disseminated infection, *B. burgdorferi* colonizes multiple tissues, leading to different clinical manifestations, including arthritis, myocarditis, and neurological and/or cutaneous abnormalities (2, 4). This acute, disseminated stage of human Lyme disease is largely recapitulated using inbred mouse strains which are susceptible to *B. burgdorferi* infection and develop carditis and subacute arthritis (5). Thus, the murine model provides a powerful tool to elucidate the role of spirochete virulence factors and host immunological responses during Lyme disease pathogenesis (4).

The *B. burgdorferi* genome encodes a large number of surface lipoproteins, many of which are expressed during mammalian infection (4, 6, 7). One of these lipoproteins is the major outer surface protein C (OspC), whose production is induced within infected nymphal ticks during feeding (8, 9). OspC continues to be produced during the early phase of infection and is highly immunogenic in mice (10, 11). As one of the strategies to evade host humoral responses, spirochetes downregulate OspC production in response to anti-OspC antibodies within 2 to 3 weeks after infection in mice (12, 13). OspC has been shown to be required for *B. burgdorferi* to establish infection in mammals (8, 14), as well as for spirochetal transmission from ticks to mammals (15, 16). Infectivity studies demonstrate that the *ospC* mutant cannot establish infection in immunocompetent and SCID mice (lacking B and T cells) when inoculated at a dose of 10^3 to 10^5 spirochetes per mouse (8, 16–20). The *ospC* mutant is cleared within the first 48 h of infection in the murine host (21), suggesting a protective role of OspC against innate defenses. The OspC protective effect in spirochetes seems to be independent of the actions of major antimicrobial peptides (22). OspC also has been proposed to play roles in promoting survival and/or dissemination of spirochetes within the mammalian host. For example, OspC binds to a tick salivary protein, Salp15, which can protect spirochetes from complement- and antibody-mediated killing (23, 24). OspC was shown to bind host plasminogen (25, 26), and this phenotype correlates with invasiveness of spirochetes in mice (27). In addition, constitutive expression of heterologous lipoproteins in the *ospC* mutant was shown to restore infection in SCID mice, suggesting that OspC

Received 24 September 2015 **Accepted** 27 September 2015

Accepted manuscript posted online 5 October 2015

Citation Carrasco SE, Troxell B, Yang Y, Brandt SL, Li H, Sandusky GE, Condon KW, Serezani CH, Yang XF. 2015. Outer surface protein OspC is an antiphagocytic factor that protects *Borrelia burgdorferi* from phagocytosis by macrophages. Infect Immun 83:4848–4860. doi:10.1128/IAI.01215-15.

Editor: A. J. Bäumler

Address correspondence to C. Henrique Serezani, hserezan@iupui.edu, or X. Frank Yang, xfyang@iupui.edu.

*Present address: Bryan Troxell, Prestage Department of Poultry Science, North Carolina State University, Raleigh, North Carolina, USA.

Supplemental material for this article may be found at http://dx.doi.org/10.1128/IAI.01215-15.

may have a nonspecific structural role for *B. burgdorferi* (14, 19). On the other hand, another study suggested that the residues within the putative ligand-binding domain are important for OspC function (25). Despite all research efforts, the precise biological function of OspC during infection remains unclear.

Innate immunity represents the first line of defense against *B. burgdorferi* infection in mammals (28, 29). Professional phagocytes, such as monocytes/macrophages and neutrophils, are among the first innate cells that spirochetes encounter during early infection at the skin site of inoculation and target tissues, such as the heart or joints, in mammals (30–32). These phagocytes are essential in controlling the spirochetal burden in tissues and directing the development of adaptive immune responses during infection in the murine host (5, 33, 34). Phagocyte recognition of *B. burgdorferi* is initiated by multiple Toll-like receptors (TLRs), including TLR2/1 heterodimers, which signal through the adaptor molecule MyD88 (myeloid differentiation primary response 88) (28). In murine models, a deficiency of MyD88 results in markedly elevated *B. burgdorferi* burdens in tissues compared to those in infected wild-type mice (33, 35). However, the *ospC* mutant remained noninfectious in MyD88$^{-/-}$ mice (36). Despite the understanding of the immune mediators that modulate host defense and inflammation in the murine model of Lyme borreliosis, the role of professional phagocytes and other innate cells in the clearance of the *ospC* mutant has not been examined.

In this study, we examined the role of OspC in the protection of spirochetes against innate cells using genetic, antibody-mediated, and pharmacological approaches. We found that the *ospC* mutant was not able to establish infection in NODSCID-*IL2r*γ^{null} and anti-Ly6G-treated SCID and C3H/HeN mice, indicating that NK cells, lytic complement, and neutrophils are not critical in the clearance of the *ospC* mutant *in vivo*. Our results showed that depletion of mononuclear phagocytes at the skin site of inoculation contribute to the clearance of the *ospC* mutant in SCID and C3H/HeN mice. We further showed that OspC plays a role for *B. burgdorferi* in macrophage phagocytosis by reducing the uptake of spirochetes by murine and human macrophages. In addition, we showed that spirochetes that overexpress OspC exhibit decreased uptake by murine macrophages. Together, our findings show that OspC protects *B. burgdorferi* strains from mononuclear phagocytes by promoting spirochetes' evasion of these innate cells during early infection in mammals.

MATERIALS AND METHODS

Bacterial strains and culture conditions. *B. burgdorferi* strain B31-A3 and the isogenic *ospC* mutant and the *ospC*-complemented strains were kindly provided by P. Rosa and K. Tilly (Rocky Mountain Laboratories, National Institute of Allergy and Infectious Diseases, National Institutes of Health) (17). AH130 is an infectious low-passage strain derived from wild-type strain 297 (37). The *ospC* mutant and the *ospAB* mutant generated in the background of *B. burgdorferi* strain 297 were reported previously (15, 38). Spirochetes were grown using standard Barbour-Stoenner-Kelly II (BSK-II) medium containing the relevant antibiotic. Cultures were maintained at 37°C and pH 7.5 in a 5% CO_2 incubator and were passaged no more than three times from the original stocks. To measure growth rate of spirochetes, cells were cultured in BSK-II medium at 37°C and pH 7.5 or pH 6.8. The cell density of cultures was monitored by counting spirochetes under a dark-field microscope (Olympus America Inc., Center Valley, PA).

Generation of GFP-expressing *B. burgdorferi* strains and the *ospAB ospC* double mutant. Wild-type *B. burgdorferi* strain B31-A3 or AH130 and the isogenic *ospC* mutants were transformed with the shuttle vector pTM61 (generously provided by G. Chaconas, University of Calgary), which harbors a gene encoding GFP under the control of a constitutive *flaB* promoter from *B. burgdorferi* (39). The same shuttle vector (pTM61) was used to transform *ospAB* and *ospAB ospC* mutant strains in the 297 background to generate GFP-expressing spirochetes. To generate an *ospAB ospC* double mutant, an *ospAB* mutant derived from AH130 strain, XY326 (38, 40), was transformed with a suicide vector pOspC-Strep plasmid (pXY302) that carries the *aadA1* cassette (which confers streptomycin resistance) (15). Electrotransformation of *B. burgdorferi* strains was performed as previously described (38). Selection for transformants was from cultures plated in a 96-well tissue culture plates (200 μl/well) containing liquid BSK-II medium and relevant antibiotic markers (50 μg ml^{-1} gentamicin, 200 μg ml^{-1} kanamycin, 50 μg ml^{-1} streptomycin, and 50 ng ml^{-1} erythromycin). Positive wells containing transformants were identified by a color change of the medium, and the presence of fluorescent spirochetes was confirmed with an Axio Imager A2 fluorescence microscope (Carl Zeiss, Jena, Germany). The complemented *ospC* mutant carrying the GFP gene was obtained by transforming the *ospC* mutant with pTM61-derived shuttle vector carrying both a GFP gene and a wild-type *ospC* gene (pSEC002; primers used to generate this construct are listed in Table S1 in the supplemental material). Transformants were visualized by fluorescence microscopy and subjected to Western blot analyses to verify the restoration of OspC (*ospC-gfp flgBp-ospC*). Plasmid profiles were performed for both the *ospC* mutant and the complemented strains, and they were identical to what was previously reported for the *ospC* mutant (15, 17).

Protein electrophoresis and immunoblotting. SDS-PAGE and immunoblotting were performed as previously described (41). Monoclonal antibodies directed against OspC, OspA, and the loading control FlaB were described previously (42), and dilutions of 1:2,000, 1:2,000, and 1:500, respectively, were used in this study.

Cell lines. The J2 retrovirus-infected alveolar macrophage cell line (AMJ2-C11) was purchased from the ATCC and grown in Dulbecco's modified Eagle's medium (DMEM) complete culture medium, as described previously (43). The human monocytic cell line THP-1 was kindly provided by J. Blum (Indiana University School of Medicine) and cultured in RPMI 1640 medium supplemented with 10% fetal bovine serum (FBS), 2 mM L-glutamine, and 1% penicillin-streptomycin solution. Cells were passaged every 3 to 4 days in fresh RPMI medium. THP-1 cells were differentiated into macrophage-like cells by culturing with 100 nM phorbol myristate acetate (PMA) in RPMI medium for 3 days as previously described (44). PMA-treated THP-1 cells were rested in fresh RPMI for 4 days more before they were used for phagocytosis assays. PMA-treated THP-1 cells were detached from the flask with nonenzymatic cell dissociation solution (Sigma-Aldrich, St. Louis, MO). HL60 human promyelocytic cell line was kindly provided by H. Broxmeyer (Indiana University School of Medicine) and differentiated into neutrophil-like cells (PMN-HL60) by culturing with 1.25% (vol/vol) dimethyl sulfoxide (DMSO) in DMEM for 6 days as previously described (45).

Isolation and immortalization of inflammatory peritoneal macrophages. Elicited murine macrophages from C57BL/6 mice were collected by peritoneal lavage with phosphate-buffered saline (PBS) 4 days after the injection of 4% thioglycolate, as described previously (46). Cells were resuspended in DMEM-conditioned medium containing 10% FBS, 10 mM HEPES, 10 ng macrophage colony-stimulating factor (M-CSF), and 1% penicillin-streptomycin–amphotericin B solution (HyClone; Thermo Scientific, Rockford, IL) and incubated in a 6-well plate (Costar, Cambridge, MA) for 12 h at 37°C with a 5% CO_2. Nonadherent cells were removed by washing the monolayers with warm serum-free medium. Adherent peritoneal macrophage monolayers were infected with the supernatants of the J2-infected cell line producing oncogenic retrovirus and mixed with DMEM-conditioned medium and 1 μg/ml Polybrene (Santa Cruz Biotechnology, Dallas, TX). After 24 h, cells were infected with a second treatment of J2 virus under the same conditions to improve transfection efficiency. Immortalized peritoneal macrophages (PMs) were ob-

tained about 4 weeks later and isolated using a previously described method (43). Residential peritoneal macrophages from C57BL/6 mice were isolated and cultured as previously described (47).

Mouse strains and inoculation with *B. burgdorferi* strains. NOD-*scid IL2rγ*^{null} mice (designated NODSCIDg mice here) were acquired from either Jackson Laboratories (Bar Harbor, ME) or the *In Vivo* Therapeutics Core at the Indiana University Simon Cancer Center (Indianapolis, IN). C.B-17 *scid* and C3H/HeN mice were acquired from either Harlan Laboratories (Indianapolis, IN) or Taconic Laboratories (Germantown, NY). Some C.B-17 *scid* mice (designated SCID mice here) and C3H/HeN mice were also from a breeding colony maintained at the Laboratory Animal Research Center (LARC) at the Indiana University School of Medicine. Mice were housed under specific-pathogen-free conditions at LARC.

For mouse infection, groups of 4- to 6-week-old C3H/HeN, SCID, and NODSCIDg were inoculated intradermally (i.d.) at the base of the tail, intraperitoneally (i.p.), or intravenously (i.v.) with a dose of either 10^3 or 10^5 spirochetes per mouse, as indicated for each experiment. Mice were euthanized at specified time points ranging from 2 days to 6 weeks postinoculation. All experiments were performed with the approval of the Indiana University Institutional Animal Care and Use Committee.

Infectivity was assessed weekly by culturing ear punch biopsy specimens in BSK-II medium supplemented with relevant antibiotic markers used to select each strain as well as the *Borrelia* antibiotic cocktail (50 μg ml^{-1} rifampin, 20 μg ml^{-1} phosphomycin, and 2.5 μg ml^{-1} amphotericin B). Cultures were evaluated for the presence of spirochetes by dark-field microscopy for up to 4 weeks before being designated negative. A single growth-positive culture occurred within 1 to 3 weeks postharvest and was used as the criterion to determine positive mouse infection.

Fluorometric phagocytosis assay. Murine PMs and PMA-treated THP-1 cells were seeded at a density of 3×10^5 cells/well in groups of 5 in 96-well tissue culture plates with opaque sides and optically clear bottoms (Costar, Corning Life Sciences, NY). On the following day, a subset of wells were preincubated for 30 min with phagocytosis inhibitor, cytochalasin D (5 μg/ml; EMD Chemicals, Gibbstown, NJ) before phagocytosis assays. PMs or PMA-treated THP-1 cells were challenged with GFP-expressing spirochetes at a multiplicity of infection (MOI) of 100:1 and coincubated at 37°C with 5% CO_2 for 2 h. Trypan blue (0.2%; Sigma-Aldrich) was added for 5 min to quench the fluorescence of extracellular bacteria, and fluorescence was determined using a Spectramax Gemini EM microplate fluorometer (Molecular Devices, Sunnyvale, CA) at excitation and emission wavelengths of 485 and 535 nm, respectively. The phagocytic index (PI) represents the fluorescence of intracellular spirochetes phagocytosed by macrophages and is expressed in relative fluorescence units as previously described (48). The PI was calculated by subtracting the fluorescence of extracellular spirochetes from cytochalasin D-treated wells from the total fluorescence of the experimental samples.

Flow cytometry. GFP-expressing spirochetes were harvested for phagocytosis assays as described above. Murine PMs, PMA-treated THP-1 cells, or PMN-HL60 cells were challenged with GFP-expressing spirochetes at an MOI of 100:1 for 2 h. Cells were washed twice in fluorescence-activated cell sorting (FACS) buffer (1× PBS, 2 mM EDTA, and 0.5% fetal calf serum [FCS]) and then fixed in FACS buffer containing 1% paraformaldehyde. Samples were analyzed using a FACSCalibur flow cytometer (BD Biosciences, San Jose, CA). To estimate the percent GFP-positive macrophages, cells were gated by forward and side scatter properties, and GFP-positive cells were identified in the FL1 channel. For flow cytometry studies using murine resident peritoneal macrophages, *B. burgdorferi*-infected cells were incubated with anti-CD16/32 (clone 93) antibodies to block the Fc receptor (eBioscience, San Diego, CA), followed by phycoerythrin (PE)-conjugated anti-mouse F4/80 (clone BM8 at a 1:200 dilution) antibodies (eBioscience). After incubation for 20 min on ice, macrophages were washed in FACS buffer and then fixed for flow-cytometric analysis. Macrophages were gated according to their expression of F4/80 antigen and identified in the FL2 channel. Cells labeled with PE-conjugated rat IgG2a (eBioscience) were used as isotype controls. Uptake of GFP-expressing spirochetes by residential macrophages was expressed as the increase in green fluorescence of F4/80$^+$ cells. Unstained cells (without GFP-expressing spirochetes) were used as negative controls for these assays. Cell debris interpreted as dead cells was excluded from analysis. Data were analyzed with Cellquest (BD Biosciences) software, and histograms were edited in FlowJo software (Tree Star, Ashland, OR).

Confocal and immunofluorescence microscopy. Murine PMs were seeded as described above and allowed to adhere to the surface of etched microscope cover slides for 4 h. PMs were then challenged with GFP-expressing spirochetes at an MOI of 100:1 and coincubated at 37°C in RPMI with 10% FBS for 2 h. Infected cells were then washed 4 times with warm PBS, fixed with 4% PFA, permeabilized with 0.1% saponin, and incubated with phalloidin conjugated with CruzFluor 647 (Santa Cruz) for F actin staining. Samples were then mounted on glass slides using ProLong Gold antifade reagent (Life Technologies, Carlsbad, CA) containing 4′,6-diamidino-2-phenylindole (DAPI) dye for cell nucleus DNA staining. Confocal imaging was performed on a Leica SP8 MP confocal microscope (Leica Microsystems Inc., Buffalo Grove, IL) at the Indiana Center of Biological Microcopy core facility. *z*-stack images were acquired using a 100× oil immersion objective at a pixel resolution of 512 by 512. Image analysis and maximum intensity projections were performed with Fiji software (Life-Line, version of 2 June 2014). Fluorescence images of infected murine PMs were obtained using a Leica DMLB fluorescence microscope (Leica Microsystems Inc.).

***In vivo* phagocyte depletions.** Dichloromethylene diphosphonate (clodronate) encapsulated in liposomes (clodronate liposomes) were purchased from www.clodronateliposomes.org (Vrije University, Amsterdam, The Netherlands). To deplete phagocytes in the skin, 50 μl of clodronate liposomes or PBS-containing liposomes (PBS liposomes, used as controls) were i.d. injected into mice 48 and 24 h before challenge with *B. burgdorferi* strains at the same treatment site. SCID and C3H/HeN mice were then i.d. and i.p. (150 μl) injected with either clodronate or PBS liposomes after 24 h postchallenge. In order to reduce recruitment of monocytes to the skin, mice were i.p. injected with either clodronate or PBS liposomes 48 h and 96 h postchallenge (49).

For neutrophil depletion studies, we used the anti-Ly6G antibody method (clone 1A8; Bio-X-Cell, West Lebanon, NH), which effectively induces neutropenia in mice (50, 51). Briefly, groups of SCID and C3H/HeN mice were treated with intraperitoneal injections of 250 μg/dose of anti-Ly6G 24 h and 2 h before wild-type B31 or *ospC* mutant challenge and 24 h postchallenge. As a comparison control group, SCID mice were injected with three doses of 250 μg each of isotype antibody rat IgG_{2a} (clone R35-95; BD Biosciences, San Jose, CA) or control rat IgG (Sigma-Aldrich).

Quantitative PCR. For quantification of *B. burgdorferi* DNA in tibiotarsal joints, total DNA was extracted from joint tissue using a DNeasy blood and tissue kit as described in the manufacturer's protocols (Qiagen, Valencia, CA). PCR quantification genomic DNA was performed using the RT^2 SYBR green ROX qPCR Mastermix (Qiagen). The oligonucleotide primer pairs used to detect *flaB* and *Nidogen* were *flaB*-XF F (forward)/*flaB*-XF R (reverse) and *Nidogen* F (forward)/*Nidogen* R (reverse), respectively (see Table S1 in the supplemental material) (38, 52) Reactions were carried out on an ABI Prism 7000 real-time PCR machine (Applied Biosystems, Pleasanton, CA). Calculations of DNA copy numbers of *flaB* were normalized with the copy numbers of the mouse *Nidogen* gene in each sample.

Leukocyte counts, histology, and immunohistochemistry (IHC). Peripheral blood from mice was collected by cardiac puncture after carbon dioxide narcosis. Complete leukocyte counts with differentials were performed using the hematology analyzer Hemavet 950FS (Drew Scientific, Oxford, CT).

For histology, skin sections (site of inoculation) were collected via 8-mm punch biopsy (Acuderm, Fort Lauderdale, FL) and fixed in 4% paraformaldehyde. Tissues were embedded in paraffin, sectioned at 5 μm,

and stained with hematoxylin and eosin (H&E). Sections were viewed on a Leica DM3000 microscope (Leica Microsystems Inc.).

Immunohistochemical staining for F4/80$^+$ cells were performed at the IHC core facility at Indiana University School of Medicine. Briefly, antigen retrieval was carried out in a Dako PT module using low-pH retrieval buffer (Dako, Carpinteria, CA). Sections were incubated with rat anti-mouse F4/80 antibody at a 1:100 dilution (AbD Serotec, Raleigh, NC) and subsequently incubated with biotinylated donkey anti-rat antibody at 1:100 dilution (Jackson ImmunoResearch, West Grove, PA). Detection was accomplished using the LSAB2 method (Dako). Of note, the F4/80 monoclonal antibody has been widely used to detect mature tissue macrophages in mice (53, 54). Thus, murine macrophages from a spleen section were used as positive controls.

To perform quantitative analysis of F4/80-stained sections, slides were scanned with an Aperio whole-slide digital imaging system (ScanScope CS; Aperio Technologies, Inc., Vista, CA). Skin sections were analyzed using the ImageScope positive pixel count algorithm. The default parameters of the positive pixel count (hue of 0.1 and width of 0.5) were used to detect F4/80$^+$ cells in sections. Data were collected by counting the number of strongly positively staining cells per high-power field and then averaging the results for three randomly selected regions (with a fixed region width of 300 pixels and height of 300 pixels) per skin section.

Similar skin sections (site of inoculation) were evaluated by Warthin-Starry staining and indirect IHC for the presence of *B. burgdorferi* using a previously described method (55, 56). Sections were incubated for 12 h at 4°C with a 1:1,000 dilution of a polyclonal immune serum from *B. burgdorferi*-immunized rabbits (generously provided by Stephen Barthold, University of California, Davis).

Statistics. Data are presented as means and standard errors of the means (SEM) and were analyzed with the Prism 5.0 statistical program (GraphPad Software). Comparisons among groups were performed with one-way analysis of variance (ANOVA) followed by a *post hoc* test, as indicated in the figure legends. Comparisons between two experimental groups were analyzed by Student's *t* test. A *P* value of <0.05 was considered significant.

RESULTS

The *ospC* mutant cannot establish infection in NODSCIDg mice deficient in lytic complement and NK, B, and T cells. Previous studies have shown that the *ospC* mutant cannot establish infection in C3H/HeN and SCID mice, which lack functional T and B cells (8, 17, 19, 21), suggesting that innate immunity is involved in clearance of *ospC* mutant spirochetes in mice. To investigate which innate factors are involved in clearance of the *ospC* mutant *in vivo*, we examined the infectivity of the *ospC* mutant in another mouse strain, NODSCIDg, which is deficient in T and B cells, as well as lacking complement C5 and functional NK cells (57). Loss of C5 prevents the activation of C5b and thereby inhibits the formation of the C5b-9 membrane attack complex (57, 58). Groups of NOD-SCIDg mice were i.d. injected with either wild-type B31-A3 or the *ospC* mutant. We used an inoculum of 10^3 spirochetes per mouse, as previously reported (8, 17, 21, 59). NODSCIDg mice were also inoculated intravenously to assess whether the injection site plays a role in the infectivity of the *ospC* mutant. As controls, groups of SCID and C3H/HeN mice were also challenged with the wild type or the *ospC* mutant. Whereas wild-type B31-A3 spirochetes were readily detectable in all tested tissues from NODSCIDg, SCID, and C3H/HeN mice after 3 weeks postchallenge, no *ospC* mutant spirochetes were detected in tissues from mice inoculated with 10^3 spirochetes per mouse (Table 1). This result is similar to results of previous studies with immunocompetent and SCID mice (8, 17, 19). The *ospC* mutant was not infectious in NODSCIDg mice even after 6 weeks postinoculation (data not shown), regardless of the route of inoculation. These results suggest that, in addition to lymphocytes, innate components such as lytic complement and NK cells are not the major factors that eliminate the *ospC* mutant *in vivo*.

TABLE 1 Infectivity of wild-type *B. burgdorferi* (B31-A3) and the isogenic *ospC* mutant in NODSCIDg, SCID, and C3H/HeN mice

Mouse type	Route of inoculation[a]	*B. burgdorferi* strain	No. of infected mice/no. tested[b]
NODSCIDg	i.d.	B31-A3	3/3
	i.d.	*ospC* mutant	0/3
	i.v.	B31-A3	3/3
	i.v.	*ospC* mutant	0/3
SCID	i.d.	B31-A3	3/3
	i.d.	*ospC* mutant	0/6
C3H/HeN	i.d.	B31-A3	3/3
	i.d.	*ospC* mutant	0/6

[a] Spirochetes were inoculated at a dose of 10^3 either intradermally (i.d.) or intravenously (i.v.) in BSK as vehicle.
[b] All mice were euthanized at 3 weeks postinoculation. Isolation of spirochetes was attempted from the skin site of inoculation, ear pinna, tibiotarsal joint, heart base, and spleen. Infectivity experiments were conducted 3 separate times.

Establishment of dose and vehicle for inoculation to study the *ospC* mutant *in vivo*. Since NODSCIDg mice have defective functions in different innate cells, we chose an immunodeficient model with an intact innate immune system, such as SCID mice, to assess the role of innate cells in clearance of the *ospC* mutant. To establish a system to study the *ospC* mutant in SCID mice, the infectious dose and the vehicle to deliver spirochetes were evaluated in a series of infectivity experiments. Spirochetes used in the infectivity studies described above were used to inoculate mice using BSK-II growth medium, which is a commonly used vehicle to test infectivity of *B. burgdorferi* strains and mutants in mice. Since BSK-II is a complex medium with 6% rabbit serum and 5% BSA (60), which may alter the host immune response at the skin site of spirochetal inoculation, we next tested whether the *ospC* mutant can establish infection using a minimal-medium vehicle, such as PBS buffer. We also compared two routes of inoculation, the intradermal and intraperitoneal routes.

Groups of SCID mice were injected with an inoculum of 10^5 of either B31-A3 or *ospC* mutant spirochetes per mouse. We increased the inoculum size to 10^5 spirochetes, since the use of PBS or saline could affect viability of spirochetes, based on our preliminary infectivity experiments (data not shown). Similar to the infectivity experiments described above, the *ospC* mutant were not detected by culture in all harvested tissues from SCID mice when 10^5 spirochetes were injected per mouse, regardless of the vehicle (PBS buffer or BSK-II medium) or the route of inoculation (i.d. or i.p.) (Table 2). Thus, we chose an inoculum of 10^5 spirochetes with PBS as a vehicle to explore the interaction of OspC-lacking spirochetes with innate host factors *in vivo*.

Phagocytes contribute to the clearance of the *ospC* mutant at the skin inoculation site. The data above, along with previous studies by others (8, 19, 36), suggest that B cells, T cells, lytic complement and NK cells were not the major host factors that eliminate the *ospC* mutant *in vivo*. We next investigated whether professional phagocytes may play a role in the clearance of the *ospC* mutant. For this purpose, we chose SCID mice, since they

TABLE 2 Infectivity of wild-type *B. burgdorferi* (B31-A3) and the *ospC* mutant in SCID mice using different vehicles and routes of inoculation

B. burgdorferi strain	Route of inoculation[a]	Vehicle	No. of infected mice/no. tested[b]
B31-A3	i.d.	PBS	3/3
	i.p.	PBS	3/3
	i.d.	BSK	3/3
ospC mutant	i.d.	PBS	0/3
	i.p.	PBS	0/3
	i.d.	BSK	0/3

[a] Spirochetes were inoculated at a dose of 10^5 either intradermally (i.d.) or intraperitoneally (i.p.).
[b] All mice were euthanized at 3 weeks postinoculation. Isolation of spirochetes was attempted from the skin site of inoculation, ear pinna, tibiotarsal joint, heart base, and spleen. Infectivity experiments were conducted two separate times.

have a functional innate immune system (58, 61). Groups of SCID mice were treated with clodronate liposome to induce depletion of phagocytes in tissues and challenged with an inoculum of 10^5 of either wild-type, *ospC* mutant, or *ospC*-complemented spirochetes. It has been extensively shown that clodronate liposome administration in the skin of mice is an effective method to deplete macrophages in the skin (54, 62). To verify the depletion of macrophages in clodronate liposome-treated mice, we performed immunohistochemistry on skin sections from each group of animals and quantified the cells that were reactive with antibody against F4/80. F4/80 is a membrane glycoprotein that is abundantly expressed on the surface of resident and activated macrophages. Every macrophage expresses F4/80+, and it has been wildly used as a pan-macrophage marker (53, 63, 64). Immunostaining of skin sections harvested 7 days postchallenge confirmed a significant reduction of phagocytes in SCID mice treated with clodronate liposomes and challenged with either wild-type, *ospC*-deficient, or *ospC*-complemented spirochetes (Fig. 1). Together, these results are in agreement with previous studies showing that subcutaneous injections of clodronate liposomes effectively deplete macrophages in mouse models of skin disorders (49, 54, 62).

To determine the effect of phagocyte depletion on the infectivity of the *ospC* mutant, we examined the presence of spirochetes in various tissues 7 days postchallenge. As expected, the *ospC* mutant could not infect the SCID mice treated with PBS liposomes (control group) (Fig. 2A and B), and the mice had neutrophil counts similar to those of naive uninfected SCID mice (see Fig. S1 in the supplemental material). In contrast, the *ospC* mutant spirochetes were now able to establish infection in SCID mice treated with clodronate (90% [9/10]). The *ospC* mutant was reisolated from skin site of inoculation, heart blood, and/or joints, and the spirochetes were detected by Warthin-Starry staining of spirochetes at the skin site of inoculation in clodronate-treated SCID mice even at day 7 postchallenge (Fig. 2B). In clodronate-treated mice, the *ospC* mutant disseminates to tissues distant from the inoculation site, and the dissemination correlated with high neutrophil counts in blood, similar to what is observed in SCID mice infected with wild-type or *ospC*-complemented spirochetes (Fig. 2A; also, see Fig. S1 in the supplemental material). Note that a low neutrophil level was observed in SCID mice infected with the *ospC*-complemented spirochetes before clodronate treatment (see Fig. S1 in the supplemental material), and the reason for this phenomenon is unclear. Nevertheless, these data suggest that macrophages play an important role in clearance of the *ospC* mutant.

To further investigate the role of phagocytes in killing of the *ospC* mutant *in vivo*, C3H/HeN mice were treated with clodronate liposomes and challenged with either wild-type, *ospC* mutant, or *ospC*-complemented strains. As expected, the *ospC* mutant was completely cleared from vehicle-treated C3H/HeN mice at day 7 postchallenge (Fig. 3A). Similar to what was observed in SCID mice, the *ospC* mutant was able to establish infection in phagocyte-depleted C3H/HeN mice (Fig. 3A; also, see Fig. S3 in the supplemental material). This group of mice exhibited high neu-

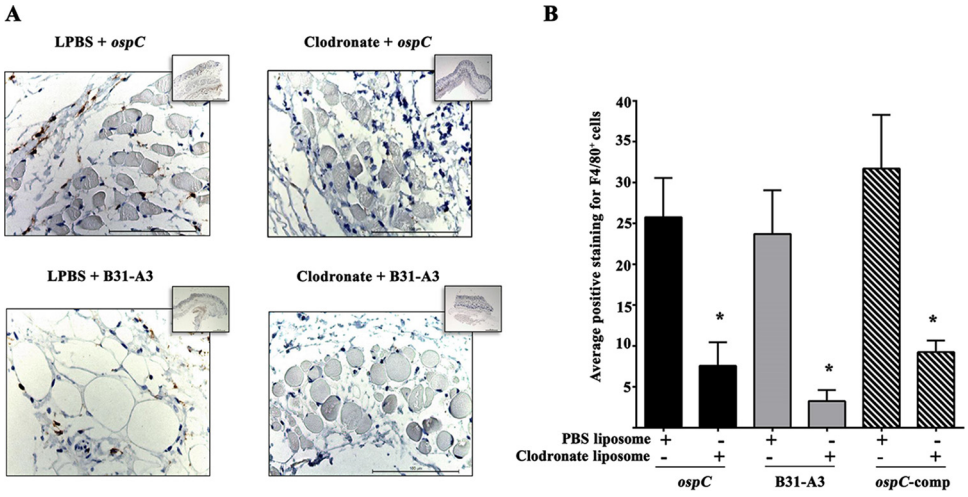

FIG 1 Clodronate liposome administration reduces the number of F4/80$^+$ phagocytes at the site of inoculation. (A) Representative images of immunohistochemical staining for detection of F4/80$^+$ cells (brown) in skin sections (magnification, ×40) from SCID mice treated with either clodronate liposomes or PBS liposomes (LPBS) 7 days after infection. Insets, 2.5× magnification showing a large area of tissue per image. (B) Quantification of F4/80$^+$ cells in the images in panel A using Aperio image analysis algorithms (the *y* axis shows the number of positively stained cells [$\times 10^3$] within the analyzed region). Data are means and SEM from skin sections (site of inoculation) from three mice per treatment condition. Three separate fixed regions were analyzed per skin section. Student's *t* test was used to determine the significance of differences between clodronate liposome treatment and PBS liposome treatment for each condition (*, $P < 0.05$).

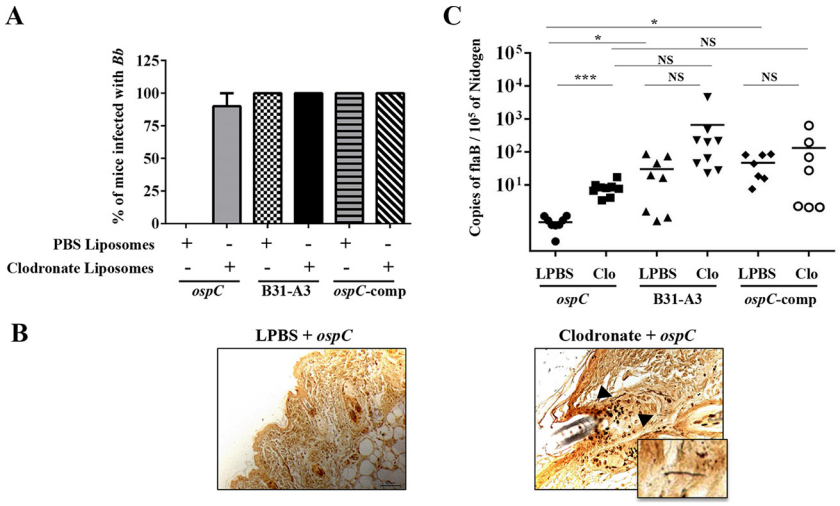

FIG 2 The *ospC* mutant disseminates and colonizes F4/80$^+$ phagocyte-depleted SCID mice. (A) Infectivity of wild-type, the *ospC* mutant, and the complemented (comp) strain (*ospC*/*ospCp-ospC*) in mice treated with either clodronate or PBS liposomes (control). The numbers of mice used in each group for the wild-type, *ospC* mutant, and complemented strains were 9, 10, and 7, respectively. Infectivity for each bacterial strain was determined from cultivation of spirochetes from the skin site of inoculation, heart blood, tibiotarsal, and ear pinna at day 7 postchallenge. (B) A representative Warthin-Starry stain demonstrating the presence of *ospC* mutant spirochetes at the skin site of inoculation (right, magnification, ×40; inset, magnification, ×100) from clodronate liposome-treated SCID mice (culture positive, $n = 5$). Spirochetes were observed in dermis (black arrows) and fasciae underneath skeletal muscle. No *ospC* mutant spirochetes were detected at the skin site of inoculation (left, magnification, ×40) of PBS liposome-treated SCID mice at day 7 postchallenge (culture negative, $n = 5$). (C) Quantitation of spirochetal burden in tibiotarsal joints of clodronate-treated mice. The isolated DNA was subjected to quantitative PCR (qPCR) analyses for the *B. burgdorferi flaB* gene and the mouse *Nidogen* gene. Data are representative of two separate experiments, and each black line indicates the mean for 7 to 10 mice in each group. Comparisons of PBS- and clodronate-treated animals were performed using unpaired Student's *t* test with Welch's correction (***, $P \leq 0.0005$; *, $P \leq 0.05$; NS, not significant).

trophil counts in blood, which was similar to results for C3H/HeN mice infected with wild-type or *ospC*-complemented spirochetes (Fig. 3A; also, see Fig. S2 in the supplemental material). Note that in mice infected with wild-type or *ospC*-complemented spirochetes, spirochetal dissemination triggered the recruitment of neutrophils in C3H/HeN mice, regardless of clodronate treatment (Fig. 3A; also, see Fig. S2 in the supplemental material), but eosinophil, basophil, and monocyte counts in the blood of these mice were not altered (data not shown). Thus, macrophage depletion in both SCID and C3H/HeN mice supports the notion that phagocytes contribute to the clearance of the *ospC* mutant *in vivo*.

Spirochetal burden in joint tissues was quantified by real-time qPCR analyses at day 7 postinfection in both SCID and C3H/HeN mice. Joints from PBS liposome-treated SCID mice infected with the *ospC* mutant did not have detectable *B. burgdorferi* DNA (Fig. 2C), which was consistent with the culture-negative results (Fig. 2A). As expected, PBS liposome-treated SCID mice infected with either the wild-type or *ospC*-complemented strain had high spirochetal loads in joints. In clodronate-treated mice, the *ospC* mutant spirochetes were readily detectable; the bacterial load seemed lower than mice infected with wild-type spirochetes, but the difference was not statistically significant (Fig. 2C). The level of wild-type spirochetes in clodronate-treated SCID mice seems higher than that in PBS-liposome-treated SCID mice, but the difference was not statistically significant (Fig. 2C). In C3H/HeN mice, clodronate liposome treatment led to significantly higher spirochetal

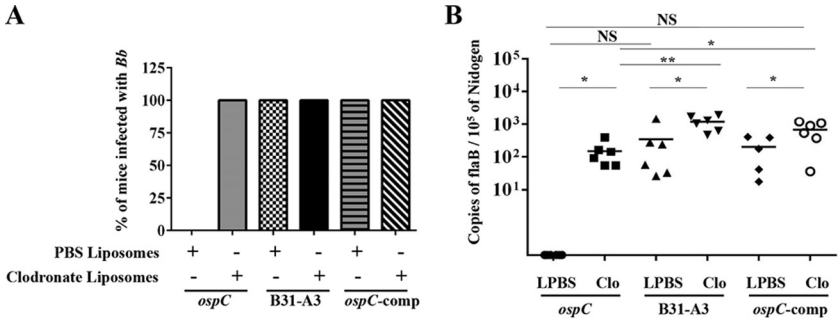

FIG 3 The *ospC* mutant disseminates and colonizes F4/80$^+$ phagocyte-depleted C3H/HeN mice. (A) Infectivity of the wild-type, *ospC* mutant, and complemented strains (*ospC*/*ospCp-ospC*) in mice treated with either clodronate or PBS liposomes (control). Six mice were used for each treatment group. Infectivity for each bacterial strain was determined from cultivation of spirochetes from the skin site of inoculation, heart blood, tibiotarsal joint, and ear pinna at day 7 postchallenge. (B) Quantitation of spirochetal burden in tibiotarsal joints of clodronate-treated mice. The isolated DNA was subjected to quantitative PCR (qPCR) analyses for the *B. burgdorferi flaB* gene and the mouse *Nidogen* gene. Data are means for five to six mice in each group. Comparisons of PBS- and clodronate-treated animals were performed using Student's *t* test with Welch's correction (**, $P \leq 0.01$; *, $P \leq 0.05$; NS, not significant).

TABLE 3 The *ospC* mutant cannot establish infection in SCID and C3H/HeN mice treated with anti-Ly6G monoclonal antibody[a]

Mouse strain	Treatment	*B. burgdorferi* strain	No. of infected mice/no. tested
SCID	Anti-Ly6G	*ospC* mutant	0/3
	Anti-Ly6G	B31-A3	3/3
	Control IgG	*ospC* mutant	0/3
	Control IgG	B31-A3	3/3
C3H/HeN	Anti-Ly6G	*ospC* mutant	0/3
	Anti-Ly6G	B31-A3	3/3
	Control IgG	*ospC* mutant	0/3
	Control IgG	B31-A3	3/3

[a] All mice were infected with *B. burgdorferi* at a dose of 10^5 and euthanized at 48 h postinoculation. Isolation of spirochetes was attempted from the skin site of inoculation, ear pinna, tibiotarsal joint, and heart blood.

loads than PBS liposome treatment for all bacterial strains (wild-type, *ospC* mutant, and *ospC*-complemented spirochetes) (Fig. 3B). Collectively, these data support the infection results showing that phagocytes were important in the clearance of the *ospC* mutant at day 7 postinfection in both SCID and C3H/HeN mice.

Treatment of mice with neutrophil-depleting antibody does not restore infectivity of the *ospC* mutant. Since neutrophils are recruited to the sites of spirochetal infection in mice (29, 30), we investigated the role of neutrophils in clearance of the *ospC* mutant. When mice were treated with a monoclonal antibody (anti-Ly6G) that specifically binds to Ly6G for neutrophil depletion *in vivo*, we found a significant reduction of circulating neutrophils in SCID and C3H/HeN after 48 h postchallenge with the *ospC* mutant (see Fig. S4 in the supplemental material). When mice were challenged with the wild-type B31-A3 strain, spirochetes were re-isolated from the skin site of inoculation and blood in anti-Ly6G and IgG-treated mice (Table 3). However, the *ospC* mutant was not able to survive at the skin site of inoculation and establish infection in anti-Ly6G and isotype IgG antibody control-treated SCID or C3H/HeN mice after the first 48 h (Table 3) and 7 days (data not shown) postchallenge. Together, these results indicate that depletion of neutrophils during the first 48 h postchallenge is not sufficient to restore the infectivity of the *ospC* mutant *in vivo*.

Abrogation of OspC increases phagocytosis by murine macrophage. The above observation that macrophages play a role in clearance of the *ospC* mutant prompted us to assess the interaction of phagocytes with spirochetes. We first generated GFP-expressing wild-type, *ospC* mutant, and *ospC*-complemented spirochetes. The immunoblotting results showed that both GFP-expressing wild-type and complemented strains (B31 and 297) were not defective in OspC expression (see Fig. S5 and S6 in the supplemental material). In addition, *in vitro* growth analysis showed that the GFP-expressing *ospC* mutant spirochetes were motile and exhibited a growth pattern similar to that of the GFP-expressing wild-type (B31) spirochetes when cultivated under various growth conditions (see Fig. S6 in the supplemental material).

Given that phagocytosis is a critical innate mechanism that macrophages employ to eliminate invading spirochetes (28), we focused on the role of OspC in macrophage phagocytosis using a fluorometry-based method which allows quantification of fluorescence of internalized microorganisms in macrophages (48, 65, 66). We found that the *ospC* mutant had approximately 75% higher phagocytosis by murine PMs than the wild-type and the *ospC*-complemented strains (Fig. 4A, left). Preliminary experiments were conducted at an MOI of 10:1 (data not shown), and assays at an MOI of 100:1 had the greatest effect on phagocytosis of the *ospC* mutant. We also confirmed this finding by using another *ospC* mutant generated in *B. burgdorferi* strain 297 (15) (Fig. 4A, right). Furthermore, we performed the flow cytometry experiment to confirm this finding, which showed that the *ospC* mutant had approximately 70% higher uptake by murine PMs than the parental wild-type spirochete (Fig. 4B).

We further visualized the enhanced uptake of the *ospC* mutant in murine PMs, we assessed fixed specimens of *B. burgdorferi* strains in contact with macrophages using immunofluorescence and confocal microscopy. When macrophages were coincubated with the GFP-expressing spirochetes for 2 h, uptake of the *ospC* mutant by PMs was enhanced compared to that of cells incubated with either the wild-type or *ospC*-complemented strain (see Fig. S7 in the supplemental material). When individual cells were examined, *ospC* spirochetes were attached to the surfaces of macrophages, enwrapped by macrophage filamentous structures and internalized in the form of fluorescent blebs or degraded amorphous fluorescent material (Fig. 4C). Fluorescent blebs or degraded fluorescent material associated with PMs was markedly decreased in cells infected with wild-type spirochetes (Fig. 4C).

To further demonstrate that OspC plays a role in preventing phagocytosis by macrophages, we isolated resident peritoneal macrophages and then performed a phagocytosis assay to analyze the percentage of GFP-expressing spirochetes ingested by macrophages by FACS analysis. We found that the population of double-positive F4/80 (marker for macrophage)- and GFP-expressing *ospC* mutant cells was significantly higher than the population of double-positive cells infected with the GFP-expressing wild-type strain (Fig. 4D). Collectively, these data suggest that spirochetes expressing OspC have an antiphagocytic property.

Abrogation of OspC increases phagocytosis by human macrophages. We examined whether spirochetes expressing OspC influence phagocytosis in human macrophage-like cells. To test this, human monocytic THP-1 cells were treated with PMA for differentiation into macrophages (44) and then used to assess phagocytosis of GFP-expressing *B. burgdorferi* strains. THP-1 human macrophage cells express an F4/80 human ortholog termed EMR1 (EGF [epidermal growth factor] module-containing, mucin-like hormone receptor 1) (67, 68). Using a fluorometric assay and FACS for phagocytosis, we found that the *ospC* mutant had significantly higher phagocytosis by PMA-treated THP-1 cells than the wild-type and the complemented spirochetes (Fig. 5A and B), similar to what was observed for mouse macrophages. We also tested whether human neutrophil-like cells have a similar function, since neutrophil is another type of professional phagocyte that can avidly phagocytose *B. burgdorferi* (69, 70). The result showed that uptake of the *ospC* mutant by human neutrophils was similar to that of the parental wild-type strain (Fig. 5C), indicating that OspC does not play a role in inhibiting neutrophil-mediated phagocytosis of spirochetes. Thus, results from both murine and human macrophages suggest that OspC has an antiphagocytic property that inhibits macrophage-mediated phagocytosis of spirochetes.

Overproduction of OspC decreases phagocytosis by macrophage. The data above demonstrate that deletion of *ospC* led to an increased phagocytosis by macrophage. To gain additional evi-

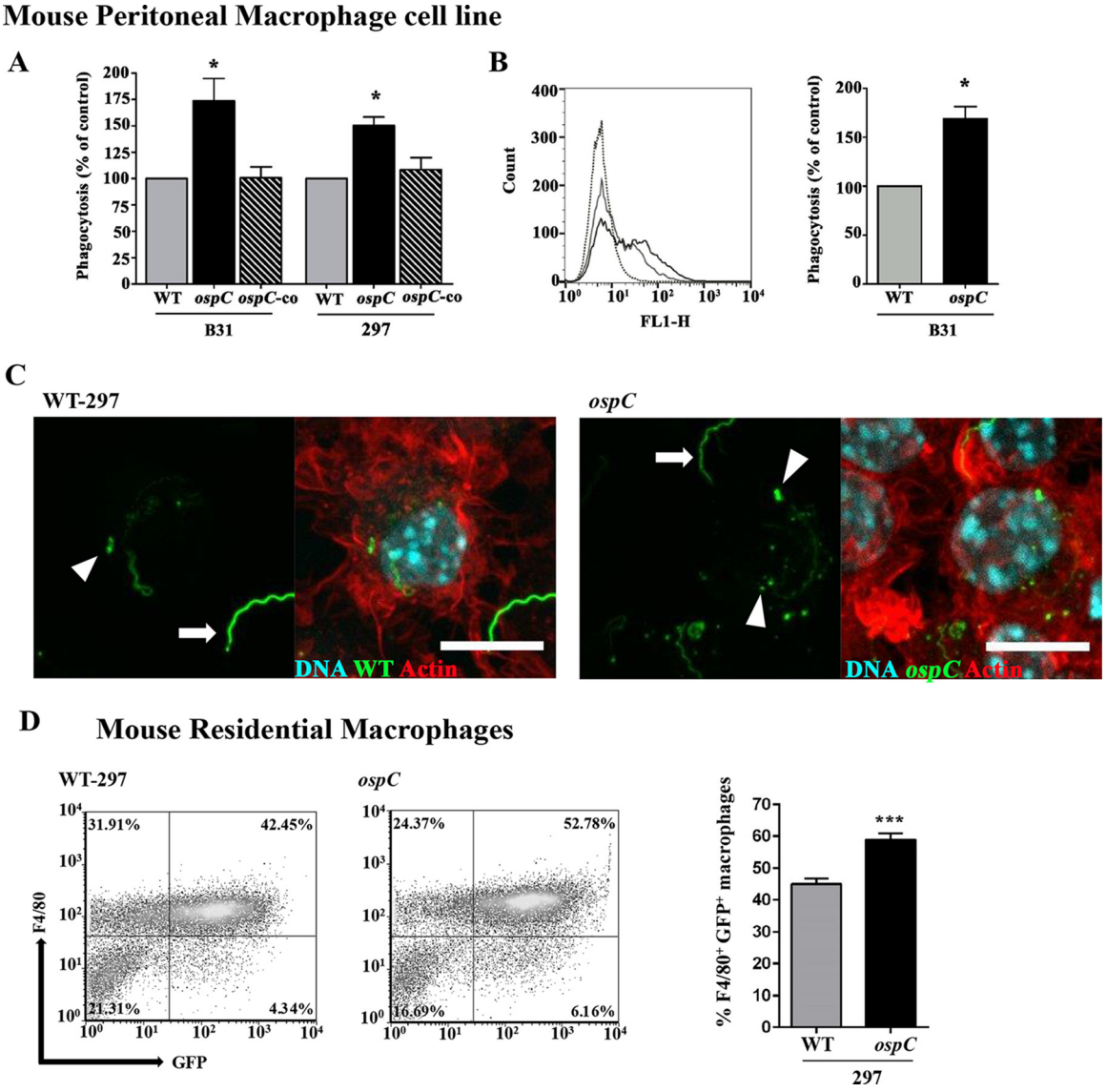

FIG 4 Abrogation of OspC enhances phagocytosis of *B. burgdorferi* by murine macrophages. (A) Quantitation of phagocytosis of GFP-expressing spirochetes (strains B31 and 297) by murine peritoneal macrophages (PMs) determined using a microplate fluorometer. PMs were incubated with GFP-expressing spirochetes at an MOI of 100 for 2 h. The phagocytic index (PI) represents the fluorescence of intracellular bacteria phagocytosed by macrophages. Data are representative of three or four separate experiments with at least 4 replicates per experiment. Values are means and SEM. Comparisons among experimental groups were performed with one-way ANOVA followed by Dunnett's *post hoc* test (*, $P < 0.05$). (B) Representative histograms of phagocytosis of B31-A3-*gfp* (gray solid line) and *ospC-gfp* (black solid line) spirochetes analyzed by flow cytometry. PMs were incubated with GFP-expressing spirochetes at an MOI of 100 for 2 h, followed by washing and fixation prior to flow-cytometric analysis. The black dotted line represents control unstained cells. The percent phagocytosis is shown on the right. Data are the percentage of GFP-expressing spirochetes phagocytosed by PMs obtained from three separate experiments (Student's *t* test; *, $P < 0.05$). Values are means and SEM. (C) Confocal *z*-stack images of murine peritoneal macrophages incubated with GFP-expressing *B. burgdorferi* spirochetes for 2 h at an MOI of 100:1. The left image shows wild-type spirochetes (strain 297) associated with a macrophage. The arrowhead indicates a bright green fluorescent bleb that appears to be internalized in a macrophage, and the arrow indicates a cell surface-associated spirochete which is mainly extracellular. The right image shows *ospC* mutant spirochetes (strain 297) associated with a macrophage. The arrowheads indicate bright fluorescent blebs that appear to have been recently internalized and/or fully degraded into a macrophage, and the arrow indicates a cell surface-associated spirochete which is in the process of being phagocytosed. Cell nucleus DNA (cyan in overlay) was stained with DAPI, and F actin (red in overlay) was stained with phalloidin (bar, 10 μm). The images are representative of three biological replicates. (D) Representative plots of murine residential peritoneal macrophages isolated from C57BL/6 mice and incubated with GFP-expressing spirochetes (wild-type strain 297 or *ospC* mutant) for 2 h at an MOI of 100:1. Macrophages were gated according to their expression of the F4/80 membrane glycoprotein. The dot plot in each upper right quadrant shows the $F4/80^+$ and GFP^+ profile for macrophages. The percent $F4/80^+$ GFP^+ residential macrophages from six mice is shown on the right. Data are the percentage of GFP-expressing spirochetes associated with $F4/80^+$ macrophages isolated from six mice (Student's *t* test; ***, $P < 0.0005$). Values are means and SEM.

dence showing that OspC plays a role in the uptake of spirochetes by macrophages, we further investigated whether overproduction of OspC would result in reduced uptake of spirochetes by macrophage. Previously, we demonstrated that an *ospAB* mutant in *B. burgdorferi* strain 297 overproduces OspC (Fig. 6A) (40). Accordingly, the *ospAB* mutant and the *ospAB ospC* double mutant were subjected to phagocytosis assays. The result showed that the *ospAB* mutant had markedly reduced uptake by murine PMs (Fig. 6B).

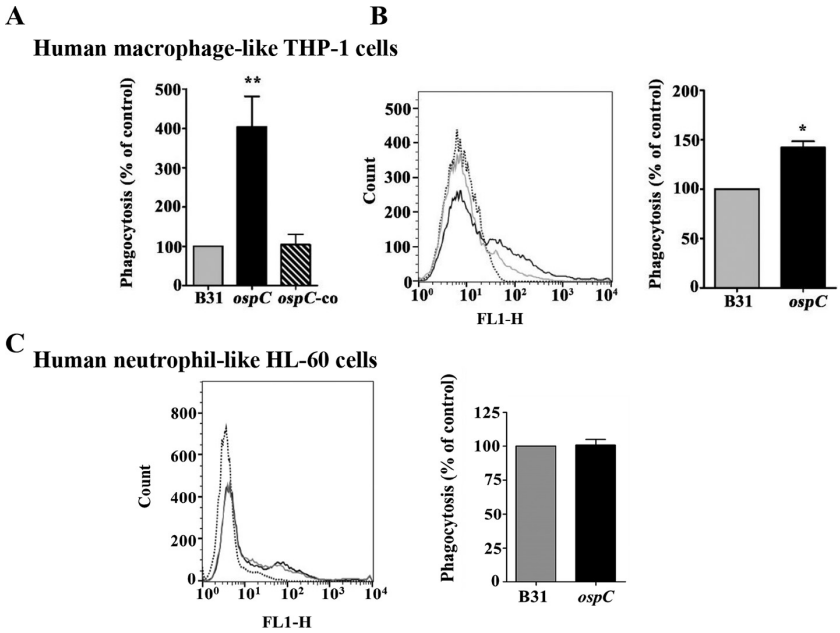

FIG 5 Abrogation of OspC enhances phagocytosis of *B. burgdorferi* by human macrophage-like cells but does not affect uptake of spirochetes by human neutrophil-like cells. (A) Quantitation of phagocytosis of GFP-expressing spirochetes (B31) by PMA-treated THP1 cells, determined by using a microplate fluorometer. PMA-treated THP-1 cells were incubated with GFP-expressing spirochetes at an MOI of 100 for 2 h. The phagocytic index (PI) represents the fluorescence of intracellular bacteria phagocytosed by PMA-treated THP1 cells. Data are representative of 3 or 4 separate experiments with at least 4 replicates per experiment. Values are means and SEM. Comparisons among experimental groups were performed with one-way ANOVA followed by Dunnett's *post hoc* test (*, $P < 0.05$; **, $P < 0.005$). (B) Representative histograms of phagocytosis of B31-A3-*gfp* (gray solid line) and *ospC-gfp* (black solid line) spirochetes analyzed by flow cytometry. PMA-treated THP-1 cells were incubated with GFP-expressing spirochetes at an MOI of 100 for 2 h, followed by washing and fixation prior to flow-cytometric analysis. The black dotted line represents control unstained cells. Percentage of phagocytosis is shown on the right. Data represent the percentage of GFP-expressing spirochetes phagocytosed by THP-1 cells obtained from three separate experiments (Student's *t* test *, $P < 0.05$). Values are means and SEM. (C) Uptake of *B. burgdorferi* by PMNHL60 cells is independent of OspC. GFP-expressing spirochetes were incubated with PMN-HL60 cells at an MOI of 100 for 2 h, followed by washing and fixation prior to flow-cytometric analysis. Representative histograms of phagocytosis of B31-A3-*gfp* (gray solid line) and *ospC-gfp* (black solid line) spirochetes analyzed by flow cytometry are shown. The black dotted line represents control unstained cells. The percent phagocytosis is shown on the right. Data are the percentage of GFP-expressing spirochetes phagocytosed by 1.25% DMSO-treated HL-60 cells obtained from three separate experiments. Values are means and SEM.

Deletion of *ospC* in the *ospAB* mutant significantly increased phagocytosis of spirochetes by murine macrophages (Fig. 6B). These results complement the results obtained from the *ospC* mutant, further supporting the notion that OspC facilitates *B. burgdorferi* to resist phagocytosis by macrophages.

DISCUSSION

The *B. burgdorferi* genome encodes numerous surface lipoproteins essential for the pathogen's successful maintenance in the enzootic life cycle (4, 7). OspC is a major surface lipoprotein that is essential for the enzootic cycle of *B. burgdorferi* (8, 15-17, 21). Although it has been proposed that OspC protects spirochetes against innate host defenses (14, 36), the mechanism how OspC contributes to such function remains elusive. In this study, we provide evidence showing that macrophages, not other components of innate immune system such as NK cells, lytic complement, or neutrophils, play a key role in the clearance of the *ospC* mutant from the skin of SCID and C3H/HeN mice during early infection. Our data showed that OspC protects spirochetes from phagocytosis by macrophage, which contributes to immune evasion of *B. burgdorferi* during the early stage of mammalian infection.

Both innate and adaptive immune responses are important to control spirochetal burden in the murine host (33, 34). Previous work has shown that the OspC-deficient spirochetes generated from different *B. burgdorferi* strain backgrounds cannot establish infection in both immunocompetent and SCID mice, indicating that adaptive immunity does not play a major role in eliminating the *ospC* mutant infection *in vivo* (8, 19). SCID mice have elevated levels of lytic complement activity and normal levels of NK cell activity (58). In this study, we further investigated NODSCIDg mice, since they lack not only adaptive immunity but also lytic complement and NK cells and also have impaired cytokine signaling due to the lack of the interleukin 2 receptor common gamma chain (IL-2Rγ^{null}) (57). Our results showed that the *ospC* mutant also was not able to establish infection in NODSCIDg mice when inoculated at the standard dose (10^3 spirochetes per mouse). The same inoculum of *ospC* mutant spirochetes cannot cause infection in C3H/HeN and SCID mice, which is what we observed in our infectivity experiments using these mouse strains (8, 17, 21, 59). Our findings suggest that the lytic complement and NK cells were dispensable in the clearance of the *ospC* mutant. These data are consistent with a previous report by Bockenstedt et al. (71), showing that the fifth component of complement is not required for protection and disease progression of wild-type *B. burgdorferi* infection in C5-deficient mouse strains. Our results also support the previous observation that depletion of NK cells did not have a major effect on *B. burgdorferi* burden and dissemination in arthritis-resistant and -susceptible mouse strains (72).

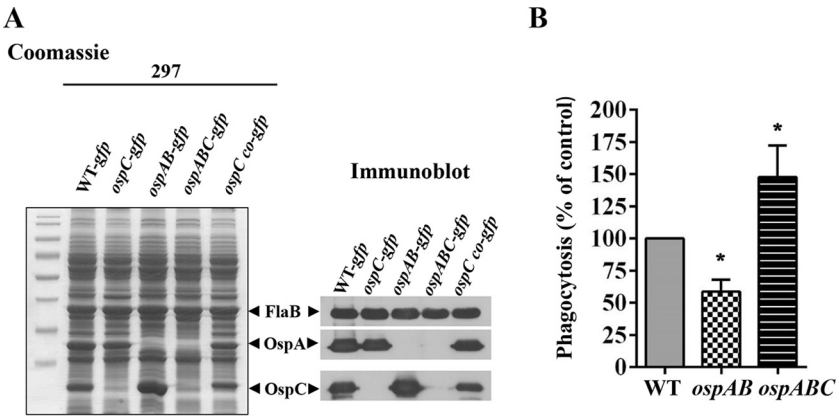

FIG 6 Overproduction of OspC decreases phagocytosis of spirochetes by macrophage. (A) Coomassie-stained gel and immunoblot showing the OspC production in GFP-expressing *B. burgdorferi* 297 strains. Wild-type (WT) infectious clone AH130 of *B. burgdorferi* strain 297, the isogenic *ospC*, *ospAB* (constitutively expressing *ospC*), and *ospABC* mutants, and the *ospC*-complemented strain were cultivated in BSK-II medium (pH 7.5) at 37°C. Spirochetes were harvested at a density of 10^8 cells/ml, and then whole-cell lysates were separated by SDS-PAGE and subjected to immunoblot analysis using a mixture of antibodies against FlaB (control), OspA, and OspC. (B) Phagocytosis of GFP-expressing wild type and the isogenic *ospAB* and *ospABC* mutants by murine PMs was measured with a microplate fluorometer. PMs were incubated with GFP-expressing spirochetes at an MOI of 100 for 2 h. The phagocytic index (PI) represents the fluorescence of intracellular bacteria phagocytosed by macrophages and was calculated as described in Material and Methods. Data are representative of 4 or 6 separate experiment with at least 4 replicates per experiment and are expressed as a percentage of phagocytosis of wild-type spirochetes (control). Values are means and SEM. Comparisons among experimental groups were performed with one-way ANOVA followed by Dunnett's *post hoc* test and Student's *t* test (*, $P < 0.05$).

In this study, we focused on professional phagocytes as one of the primary target cells for our depletion studies, as phagocytes were reported to infiltrate the skin site of inoculation or to be elevated systemically in mice infected with *B. burgdorferi* (59, 73). Our result showed that the *ospC* mutant was cleared within the first 48 h postchallenge in neutropenic SCID and C3H/HeN mice. Although previous reports showed that neutrophils effectively control spirochete burden in tissues from mice infected with wild-type spirochetes (74, 75), our data indicated that neutrophils were not the major factor in clearing the *ospC* mutant at the skin site of inoculation in mice. This finding is consistent with a previous study showing no differences in neutrophil infiltration in skin biopsy specimens from mice challenged with wild-type or *ospC* mutant spirochetes (59). In contrast, we found that depletion of mononuclear phagocytes at the skin site of inoculation in SCID and C3H/HeN mice allowed the *ospC* mutant to establish infection and dissemination, suggesting that these innate cells were indispensable in clearing the *ospC* mutant. This result implies that *B. burgdorferi* employs OspC to resist mononuclear phagocyte killing at the skin site of infection. We also observed an increased spirochete load in joints of clodronate liposome-treated mice, which is consistent with the notion that mononuclear phagocytes are important in controlling *B. burgdorferi* burden in cardiac tissue and joints of infected mice (30, 33). However, the spirochete load in joints of clodronate liposome-treated mice infected with the *ospC* mutant was still lower than the spirochete load from joints of treated mice infected with either the wild-type or *ospC*-complemented strain. This observation suggests that either ablation of multiple innate host factors is needed to restore comparable spirochete loads in tissues between the *ospC* mutant and the wild-type strain or the *ospC* mutant had a defect in the ability to adapt and replicate in mouse skin, regardless of the innate immune pressure on *ospC* spirochetes.

Administration of clodronate liposome is an effective approach to deplete mononuclear phagocytes such as macrophages from the skin in mice (54, 62, 76). One caveat for this approach is that it relies on the mode of action of clodronate bisphosphonate to induce apoptosis inside the cells, which can have an anti-inflammatory effect in tissue milieus and alter the innate cell homeostasis (77, 78). Although apoptosis was not quantified from skin biopsy specimens used in this study, we observed apoptotic cells on skin sections (data not shown), which may have created a permissive environment for the *ospC* mutant to survive at the skin site of inoculation in treated mice and may also indirectly contribute to the *ospC* mutant to establish infection in mice. The role of ingestion of spirochete-infected apoptotic cells in the clearance of *B. burgdorferi* remains to be investigated. In addition, although clodronate liposome administration in the skin of mice is an effective and selective method to deplete macrophages in the skin (54, 62), other phagocytes, including dendritic cells (DCs), may also be depleted. Although we were not able to determine the contribution of DCs to the clearance of *ospC* mutant, our subsequent *in vitro* data demonstrated that resident macrophages play an important role in phagocytosis of the *ospC* mutant.

Human macrophages and murine peritoneal and bone marrow-derived macrophages can efficiently phagocytose and kill *B. burgdorferi* (79, 80). In addition, *B. burgdorferi* encodes complement regulator-acquiring surface proteins (CRASPs), which provides resistance to complement activation that leads to a reduction in phagocytosis (81, 82). In our phagocytosis assays, we demonstrated significantly higher nonopsonic phagocytosis of the *ospC* mutant than the wild-type strain using two independent *B. burgdorferi* infectious strains and murine and human macrophages. We also incubated macrophages with recombinant OspC prior to the phagocytosis assay but did not observe a reduction in the uptake of spirochetes by murine peritoneal macrophages (data not shown). One possible explanation is that recombinant OspC is not lipidated. Unfortunately, expressing lipidated recombinant OspC is technically challenging, and we have not been able to obtain such a protein. Another possible explanation is that recombinant OspC may not be folded correctly and may therefore fail to be recognized by a phagocytic receptor.

To obtain additional evidence that OspC is involved in phagocytosis, we examined the phagocytosis of an *B. burgdorferi* strain that constitutively overproduces OspC, the *ospAB* mutant. OspA and OspB are two proteins encoded by a single operon on linear plasmid 54 (83) and are primarily expressed in the tick vector but repressed during a blood meal, when spirochetes prepare to infect mammals (38, 84, 85). We previously generated an *ospAB* mutant of strain 297 that constitutively produces high level of *ospC*. This *ospAB* mutant strain remained infectious and caused arthritis in mice (38). We found that this strain was significantly less phagocytosed by murine peritoneal macrophages, which further supports previous reports showing that OspC has a protective role in spirochetes facing innate defenses *in vivo*.

In this study, we showed that PMA-differentiated THP-1 cells were highly phagocytic against a *B. burgdorferi ospC* mutant strain, which is different from a previous study showing that vitamin D_3-treated THP-1 cells had poor phagocytic capacity for *B. burgdorferi* (86). One possible explanation was that we used PMA to activate and differentiate THP-1 cells into macrophage-like cells (87, 88). PMA-differentiated THP-1 cells have been demonstrated to exhibit higher phagocytic activity and adherence and different expression of surface receptors than vitamin D_3-differentiated THP-1 cells (44, 88).

In conclusion, our findings reveal a novel antiphagocytic property for OspC which may facilitate the evasion of spirochetes from mononuclear phagocytes during early mammalian infection. In addition, since OspC is upregulated when spirochetes are in the tick midgut during the process of tick feeding, OspC could protect *B. burgdorferi* from phagocytosis in the tick vector. Although several major surface proteins of *B. burgdorferi* have been shown to play roles in interactions with host factors (e.g., DbpB/A, BBK32, and Lmp) (66, 89, 90), none of these proteins were reported to have the antiphagocytic activity of a major borrelial surface protein. We are currently delineating the underlying mechanism by which OspC affects phagocytosis by macrophage. In this regard, it is known that phagocytosis of *B. burgdorferi* by macrophages involves several phagocytic receptors (91–93) and pattern recognition receptors (28, 94). One possibility is that OspC alters phagocytic receptor profiles upon contact with macrophages. Alternatively, OspC may shield *Borrelia* ligands from interacting with phagocytosis by macrophage via conventional (28) or coiling phagocytosis (79). Our findings implicate that mononuclear phagocytes, including macrophages, may serve as a natural barrier contributing to control *B. burgdorferi* numbers at the skin site of inoculation, which subsequently influences the outcome of spirochetal invasiveness in the murine host.

ACKNOWLEDGMENTS

We acknowledge Patricia Rosa and Kit Tilly for *B. burgdorferi* strains, George Chaconas and Tara Moriarty for pTM61 plasmid, Constance Temm (IUSM Immunohistochemistry Core) for assistance with F4/80 immunostaining, and Stephen Barthold and Denise Imai for immunohistochemical protocol and rabbit immune sera against *B. burgdorferi* lysate. Confocal imaging was performed at the Indiana Center of Biological Microcopy core facility, with the assistance of Seth Winfree.

Funding for this work was partially provided by NIH grants 2R01AI083640 and 1R21AI117198 (to X.F.Y.), HL-103777 and HL-124159 (to C.H.S.), and Indiana INGEN and METACyt grants from Indiana University, funded by the Lilly Endowment, Inc. (to X.F.Y.). Trainees S.E.C. and S.L.B. were supported by the NIH, NRSA T32 AI 060519, Immunology and Infectious Disease Program at IUSM. This investigation was partially conducted in a facility with support from research facilities improvement program grant number C06 RR015481-01 from the National Center for Research Resources, NIH.

We have no conflicts of interest.

REFERENCES

1. **Centers for Disease Control and Prevention (CDC).** 2012. Summary of notifiable disease—United States 2011. MMWR Morb Mortal Wkly Rep **60:**26.
2. **Steere AC, Grodzicki RL, Kornblatt AN, Craft JE, Barbour AG, Burgdorfer W, Schmid GP, Johnson E, Malawista SE.** 1983. The spirochetal etiology of Lyme disease. N Engl J Med **308:**733–740. http://dx.doi.org/10.1056/NEJM198303313081301.
3. **Steere AC, Coburn J, Glickstein L.** 2004. The emergence of Lyme disease. J Clin Invest **113:**1093–1101. http://dx.doi.org/10.1172/JCI21681.
4. **Radolf JD, Caimano MJ, Stevenson B, Hu LT.** 2012. Of ticks, mice and men: understanding the dual-host lifestyle of Lyme disease spirochaetes. Nat Rev Microbiol **10:**87–99. http://dx.doi.org/10.1038/nrmicro2714.
5. **Barthold SW, Sidman CL, Smith AL.** 1992. Lyme borreliosis in genetically resistant and susceptible mice with severe combined immunodeficiency. Am J Trop Med Hyg **47:**605–613.
6. **Samuels DS.** 2011. Gene regulation in *Borrelia burgdorferi*. Annu Rev Microbiol **65:**479–499. http://dx.doi.org/10.1146/annurev.micro.112408.134040.
7. **Kenedy MR, Lenhart TR, Akins DR.** 2012. The role of *Borrelia burgdorferi* outer surface proteins. FEMS Immunol Med Microbiol **66:**1–19. http://dx.doi.org/10.1111/j.1574-695X.2012.00980.x.
8. **Grimm D, Tilly K, Byram R, Stewart PE, Krum JG, Bueschel DM, Schwan TG, Policastro PF, Elias AF, Rosa PA.** 2004. Outer-surface protein C of the Lyme disease spirochete: a protein induced in ticks for infection of mammals. Proc Natl Acad Sci U S A **101:**3142–3147. http://dx.doi.org/10.1073/pnas.0306845101.
9. **Schwan TG, Piesman J, Golde WT, Dolan MC, Rosa PA.** 1995. Induction of an outer surface protein on *Borrelia burgdorferi* during tick feeding. Proc Natl Acad Sci U S A **92:**2909–2913. http://dx.doi.org/10.1073/pnas.92.7.2909.
10. **Bockenstedt LK, Hodzic E, Feng S, Bourrel KW, de Silva A, Montgomery RR, Fikrig E, Radolf JD, Barthold SW.** 1997. *Borrelia burgdorferi* strain-specific OspC-mediated immunity in mice. Infect Immun **65:**4661–4667.
11. **Gilmore RD, Jr, Kappel KJ, Dolan MC, Burkot TR, Johnson BJ.** 1996. Outer surface protein C (OspC), but not P39, is a protective immunogen against a tick-transmitted *Borrelia burgdorferi* challenge: evidence for a conformational protective epitope in OspC. Infect Immun **64:**2234–2239.
12. **Liang FT, Jacobs MB, Bowers LC, Philipp MT.** 2002. An immune evasion mechanism for spirochetal persistence in Lyme borreliosis. J Exp Med **195:**415–422. http://dx.doi.org/10.1084/jem.20011870.
13. **Liang FT, Yan J, Mbow ML, Sviat SL, Gilmore RD, Mamula M, Fikrig E.** 2004. *Borrelia burgdorferi* changes its surface antigenic expression in response to host immune responses. Infect Immun **72:**5759–5767. http://dx.doi.org/10.1128/IAI.72.10.5759-5767.2004.
14. **Radolf JD, Caimano MJ.** 2008. The long strange trip of *Borrelia burgdorferi* outer-surface protein C. Mol Microbiol **69:**1–4. http://dx.doi.org/10.1111/j.1365-2958.2008.06226.x.
15. **Pal U, Yang X, Chen M, Bockenstedt LK, Anderson JF, Flavell RA, Norgard MV, Fikrig E.** 2004. OspC facilitates *Borrelia burgdorferi* invasion of *Ixodes scapularis* salivary glands. J Clin Invest **113:**220–230. http://dx.doi.org/10.1172/JCI200419894.
16. **Fingerle V, Goettner G, Gern L, Wilske B, Schulte-Spechtel U.** 2007. Complementation of a *Borrelia afzelii* OspC mutant highlights the crucial role of OspC for dissemination of *Borrelia afzelii* in *Ixodes ricinus*. Int J Med Microbiol **297:**97–107. http://dx.doi.org/10.1016/j.ijmm.2006.11.003.
17. **Tilly K, Krum JG, Bestor A, Jewett MW, Grimm D, Bueschel D, Byram R, Dorward D, VanRaden MJ, Stewart P, Rosa P.** 2006. *Borrelia burgdorferi* OspC protein required exclusively in a crucial early stage of mammalian infection. Infect Immun **74:**3554–3564. http://dx.doi.org/10.1128/IAI.01950-05.
18. **Xu Q, McShan K, Liang FT.** 2007. Identification of an ospC operator critical for immune evasion of Borrelia burgdorferi. Mol Microbiol **64:**220–231. http://dx.doi.org/10.1111/j.1365-2958.2007.05636.x.
19. **Xu Q, McShan K, Liang FT.** 2008. Essential protective role attributed to the

surface lipoproteins of *Borrelia burgdorferi* against innate defences. Mol Microbiol **69:**15–29. http://dx.doi.org/10.1111/j.1365-2958.2008.06264.x.
20. **Gilbert MA, Morton EA, Bundle SF, Samuels DS.** 2007. Artificial regulation of ospC expression in *Borrelia burgdorferi*. Mol Microbiol **63:**1259–1273. http://dx.doi.org/10.1111/j.1365-2958.2007.05593.x.
21. **Tilly K, Bestor A, Jewett MW, Rosa P.** 2007. Rapid clearance of Lyme disease spirochetes lacking OspC from skin. Infect Immun **75:**1517–1519. http://dx.doi.org/10.1128/IAI.01725-06.
22. **Sarkar A, Tilly K, Stewart P, Bestor A, Battisti JM, Rosa PA.** 2009. *Borrelia burgdorferi* resistance to a major skin antimicrobial peptide is independent of outer surface lipoprotein content. Antimicrob Agents Chemother **53:**4490–4494. http://dx.doi.org/10.1128/AAC.00558-09.
23. **Hovius JW, Schuijt TJ, de Groot KA, Roelofs JJ, Oei GA, Marquart JA, de Beer R, van't Veer C, van der Poll T, Ramamoorthi N, Fikrig E, van Dam AP.** 2008. Preferential protection of *Borrelia burgdorferi* sensu stricto by a Salp15 homologue in Ixodes ricinus saliva. J Infect Dis **198:**1189–1197. http://dx.doi.org/10.1086/591917.
24. **Schuijt TJ, Hovius JW, van Burgel ND, Ramamoorthi N, Fikrig E, van Dam AP.** 2008. The tick salivary protein Salp15 inhibits the killing of serum-sensitive *Borrelia burgdorferi* sensu lato isolates. Infect Immun **76:**2888–2894. http://dx.doi.org/10.1128/IAI.00232-08.
25. **Earnhart CG, Leblanc DV, Alix KE, Desrosiers DC, Radolf JD, Marconi RT.** 2010. Identification of residues within ligand-binding domain 1 (LBD1) of the *Borrelia burgdorferi* OspC protein required for function in the mammalian environment. Mol Microbiol **76:**393–408. http://dx.doi.org/10.1111/j.1365-2958.2010.07103.x.
26. **Onder O, Humphrey PT, McOmber B, Korobova F, Francella N, Greenbaum DC, Brisson D.** 2012. OspC is potent plasminogen receptor on surface of *Borrelia burgdorferi*. J Biol Chem **287:**16860–16868. http://dx.doi.org/10.1074/jbc.M111.290775.
27. **Lagal V, Portnoi D, Faure G, Postic D, Baranton G.** 2006. *Borrelia burgdorferi* sensu stricto invasiveness is correlated with OspC-plasminogen affinity. Microbes Infect **8:**645–652. http://dx.doi.org/10.1016/j.micinf.2005.08.017.
28. **Cervantes JL, Hawley KL, Benjamin SJ, Weinerman B, Luu SM, Salazar JC.** 2014. Phagosomal TLR signaling upon *Borrelia burgdorferi* infection. Front Cell Infect Microbiol **4:**55. http://dx.doi.org/10.3389/fcimb.2014.00055.
29. **Montgomery RR, Lusitani D, de Boisfleury Chevance A, Malawista SE.** 2002. Human phagocytic cells in the early innate immune response to *Borrelia burgdorferi*. J Infect Dis **185:**1773–1779. http://dx.doi.org/10.1086/340826.
30. **Montgomery RR, Booth CJ, Wang X, Blaho VA, Malawista SE, Brown CR.** 2007. Recruitment of macrophages and polymorphonuclear leukocytes in L:yme carditis. Infect Immun **75:**613–620. http://dx.doi.org/10.1128/IAI.00685-06.
31. **Steere AC, Glickstein L.** 2004. Elucidation of Lyme arthritis. Nat Rev Immunol **4:**143–152. http://dx.doi.org/10.1038/nri1267.
32. **Lusitani D, Malawista SE, Montgomery RR.** 2002. *Borrelia burgdorferi* are susceptible to killing by a variety of human polymorphonuclear leukocyte components. J Infect Dis **185:**797–804. http://dx.doi.org/10.1086/339341.
33. **Bolz DD, Sundsbak RS, Ma Y, Akira S, Kirschning CJ, Zachary JF, Weis JH, Weis JJ.** 2004. MyD88 plays a unique role in host defense but not arthritis development in Lyme disease. J Immunol **173:**2003–2010. http://dx.doi.org/10.4049/jimmunol.173.3.2003.
34. **Wooten RM, Weis JJ.** 2001. Host-pathogen interactions promoting inflammatory Lyme arthritis: use of mouse models for dissection of disease processes. Curr Opin Microbiol **4:**274–279. http://dx.doi.org/10.1016/S1369-5274(00)00202-2.
35. **Behera AK, Hildebrand E, Bronson RT, Perides G, Uematsu S, Akira S, Hu LT.** 2006. MyD88 deficiency results in tissue-specific changes in cytokine induction and inflammation in interleukin-18-independent mice infected with *Borrelia burgdorferi*. Infect Immun **74:**1462–1470. http://dx.doi.org/10.1128/IAI.74.3.1462-1470.2006.
36. **Stewart PE, Wang X, Bueschel DM, Clifton DR, Grimm D, Tilly K, Carroll JA, Weis JJ, Rosa PA.** 2006. Delineating the requirement for the *Borrelia burgdorferi* virulence factor OspC in the mammalian host. Infect Immun **74:**3547–3553. http://dx.doi.org/10.1128/IAI.00158-06.
37. **Hughes CA, Kodner CB, Johnson RC.** 1992. DNA analysis of *Borrelia burgdorferi* NCH-1, the first northcentral U.S. human Lyme disease isolate. J Clin Microbiol **30:**698–703.
38. **Yang XF, Pal U, Alani SM, Fikrig E, Norgard MV.** 2004. Essential role for OspA/B in the life cycle of the Lyme disease spirochete. J Exp Med **199:**641–648. http://dx.doi.org/10.1084/jem.20031960.
39. **Moriarty TJ, Norman MU, Colarusso P, Bankhead T, Kubes P, Chaconas G.** 2008. Real-time high resolution 3D imaging of the Lyme disease spirochete adhering to and escaping from the vasculature of a living host. PLoS Pathog **4:**e1000090. http://dx.doi.org/10.1371/journal.ppat.1000090.
40. **He M, Oman T, Xu H, Blevins J, Norgard MV, Yang XF.** 2008. Abrogation of ospAB constitutively activates the Rrp2-RpoN-RpoS pathway (sigmaN-sigmaS cascade) in *Borrelia burgdorferi*. Mol Microbiol **70:**1453–1464. http://dx.doi.org/10.1111/j.1365-2958.2008.06491.x.
41. **Ye M, Zhang JJ, Fang X, Lawlis GB, Troxell B, Zhou Y, Gomelsky M, Lou Y, Yang XF.** 2014. DhhP, a cyclic di-AMP phosphodiesterase of *Borrelia burgdorferi*, is essential for cell growth and virulence. Infect Immun **82:**1840–1849. http://dx.doi.org/10.1128/IAI.00030-14.
42. **Yang X, Goldberg MS, Popova TG, Schoeler GB, Wikel SK, Hagman KE, Norgard MV.** 2000. Interdependence of environmental factors influencing reciprocal patterns of gene expression in virulent *Borrelia burgdorferi*. Mol Microbiol **37:**1470–1479. http://dx.doi.org/10.1046/j.1365-2958.2000.02104.x.
43. **Zhou H, Imrich A, Kobzik L.** 2008. Characterization of immortalized MARCO and SR-AI/II-deficient murine alveolar macrophage cell lines. Part Fibre Toxicol **5:**7. http://dx.doi.org/10.1186/1743-8977-5-7.
44. **Daigneault M, Preston JA, Marriott HM, Whyte MK, Dockrell DH.** 2010. The identification of markers of macrophage differentiation in PMA-stimulated THP-1 cells and monocyte-derived macrophages. PLoS One **5:**e8668. http://dx.doi.org/10.1371/journal.pone.0008668.
45. **Birnie GD.** 1988. The HL60 cell line: a model system for studying human myeloid cell differentiation. Br J Cancer Suppl **9:**41–45.
46. **Serezani CH, Perrela JH, Russo M, Peters-Golden M, Jancar S.** 2006. Leukotrienes are essential for the control of Leishmania amazonensis infection and contribute to strain variation in susceptibility. J Immunol **177:**3201–3208. http://dx.doi.org/10.4049/jimmunol.177.5.3201.
47. **Filgueiras LR, Brandt SL, Wang S, Wang Z, Morris DL, Evans-Molina C, Mirmira RG, Jancar S, Serezani CH.** 2015. Leukotriene B4-mediated sterile inflammation promotes susceptibility to sepsis in a mouse model of type 1 diabetes. Sci Signal **8:**ra10. http://dx.doi.org/10.1126/scisignal.2005568.
48. **Aronoff DM, Canetti C, Peters-Golden M.** 2004. Prostaglandin E2 inhibits alveolar macrophage phagocytosis through an E-prostanoid 2 receptor-mediated increase in intracellular cyclic AMP. J Immunol **173:**559–565. http://dx.doi.org/10.4049/jimmunol.173.1.559.
49. **Mishalian I, Ordan M, Peled A, Maly A, Eichenbaum MB, Ravins M, Aychek T, Jung S, Hanski E.** 2011. Recruited macrophages control dissemination of group A Streptococcus from infected soft tissues. J Immunol **187:**6022–6031. http://dx.doi.org/10.4049/jimmunol.1101385.
50. **Daley JM, Thomay AA, Connolly MD, Reichner JS, Albina JE.** 2008. Use of Ly6G-specific monoclonal antibody to deplete neutrophils in mice. J Leukoc Biol **83:**64–70.
51. **Shi C, Hohl TM, Leiner I, Equinda MJ, Fan X, Pamer EG.** 2011. Ly6G+ neutrophils are dispensable for defense against systemic Listeria monocytogenes infection. J Immunol **187:**5293–5298. http://dx.doi.org/10.4049/jimmunol.1101721.
52. **Morrison TB, Ma Y, Weis JH, Weis JJ.** 1999. Rapid and sensitive quantification of Borrelia burgdorferi-infected mouse tissues by continuous fluorescent monitoring of PCR. J Clin Microbiol **37:**987–992.
53. **Austyn JM, Gordon S.** 1981. F4/80, a monoclonal antibody directed specifically against the mouse macrophage. Eur J Immunol **11:**805–815. http://dx.doi.org/10.1002/eji.1830111013.
54. **Wang H, Peters T, Kess D, Sindrilaru A, Oreshkova T, Van Rooijen N, Stratis A, Renkl AC, Sunderkotter C, Wlaschek M, Haase I, Scharffetter-Kochanek K.** 2006. Activated macrophages are essential in a murine model for T cell-mediated chronic psoriasiform skin inflammation. J Clin Invest **116:**2105–2114. http://dx.doi.org/10.1172/JCI27180.
55. **Barthold SW, Hodzic E, Tunev S, Feng S.** 2006. Antibody-mediated disease remission in the mouse model of Lyme borreliosis. Infect Immun **74:**4817–4825. http://dx.doi.org/10.1128/IAI.00469-06.
56. **Aberer E, Duray PH.** 1991. Morphology of *Borrelia burgdorferi*: structural patterns of cultured borreliae in relation to staining methods. J Clin Microbiol **29:**764–772.
57. **Shultz LD, Lyons BL, Burzenski LM, Gott B, Chen X, Chaleff S, Kotb M, Gillies SD, King M, Mangada J, Greiner DL, Handgretinger R.** 2005. Human lymphoid and myeloid cell development in NOD/LtSz-scid IL2R gamma null mice engrafted with mobilized human hemopoietic stem cells. J Immunol **174:**6477–6489. http://dx.doi.org/10.4049/jimmunol.174.10.6477.

58. **Shultz LD, Schweitzer PA, Christianson SW, Gott B, Schweitzer IB, Tennent B, McKenna S, Mobraaten L, Rajan TV, Greiner DL, Leiter EH.** 1995. Multiple defects in innate and adaptive immunologic function in NOD/LtSz-scid mice. J Immunol **154:**180–191.
59. **Antonara S, Ristow L, McCarthy J, Coburn J.** 2010. Effect of *Borrelia burgdorferi* OspC at the site of inoculation in mouse skin. Infect Immun **78:**4723–4733. http://dx.doi.org/10.1128/IAI.00464-10.
60. **Barbour AG.** 1984. Isolation and cultivation of Lyme disease spirochetes. Yale J Biol Med **57:**521–525.
61. **Wherry JC, Schreiber RD, Unanue ER.** 1991. Regulation of gamma interferon production by natural killer cells in scid mice: roles of tumor necrosis factor and bacterial stimuli. Infect Immun **59:**1709–1715.
62. **Chow A, Brown BD, Merad M.** 2011. Studying the mononuclear phagocyte system in the molecular age. Nat Rev Immunol **11:**788–798. http://dx.doi.org/10.1038/nri3087.
63. **Murray PJ, Wynn TA.** 2011. Protective and pathogenic functions of macrophage subsets. Nat Rev Immunol **11:**723–737. http://dx.doi.org/10.1038/nri3073.
64. **Ginhoux F, Merad M.** 2010. Ontogeny and homeostasis of Langerhans cells. Immunol Cell Biol **88:**387–392. http://dx.doi.org/10.1038/icb.2010.38.
65. **Thelen T, Hao Y, Medeiros AI, Curtis JL, Serezani CH, Kobzik L, Harris LH, Aronoff DM.** 2010. The class A scavenger receptor, macrophage receptor with collagenous structure, is the major phagocytic receptor for Clostridium sordellii expressed by human decidual macrophages. J Immunol **185:**4328–4335. http://dx.doi.org/10.4049/jimmunol.1000989.
66. **Benoit VM, Fischer JR, Lin Y-P, Parveen N, Leong JM.** 2011. Allelic variation of the Lyme disease spirochete adhesin DbpA influences spirochetal binding to decorin, dermatan sulfate, and mammalian cells. Infect Immun **79:**3501–3509. http://dx.doi.org/10.1128/IAI.00163-11.
67. **Gordon S, Hamann J, Lin HH, Stacey M.** 2011. F4/80 and the related adhesion-GPCRs. Eur J Immunol **41:**2472–2476. http://dx.doi.org/10.1002/eji.201141715.
68. **Luciani N, Gazeau F, Wilhelm C.** 2009. Reactivity of the monocyte/macrophage system to superparamagnetic anionic nanoparticles. J Mater Chem **19:**6373–6380. http://dx.doi.org/10.1039/b903306h.
69. **Rittig MG, Krause A, Haupl T, Schaible UE, Modolell M, Kramer MD, Lutjen-Drecoll E, Simon MM, Burmester GR.** 1992. Coiling phagocytosis is the preferential phagocytic mechanism for *Borrelia burgdorferi*. Infect Immun **60:**4205–4212.
70. **Suhonen J, Hartiala K, Tuominen-Gustafsson H, Viljanen MK.** 2000. Borrelia burgdorferi-induced oxidative burst, calcium mobilization, and phagocytosis of human neutrophils are complement dependent. J Infect Dis **181:**195–202. http://dx.doi.org/10.1086/315195.
71. **Bockenstedt LK, Barthold S, Deponte K, Marcantonio N, Kantor FS.** 1993. *Borrelia burgdorferi* infection and immunity in mice deficient in the fifth component of complement. Infect Immun **61:**2104–2107.
72. **Brown CR, Reiner SL.** 1998. Activation of natural killer cells in arthritis-susceptible but not arthritis-resistant mouse strains following *Borrelia burgdorferi* infection. Infect Immun **66:**5208–5214.
73. **Barthold SW, Persing DH, Armstrong AL, Peeples RA.** 1991. Kinetics of *Borrelia burgdorferi* dissemination and evolution of disease after intradermal inoculation of mice. Am J Pathol **139:**263–273.
74. **Brown CR, Blaho VA, Loiacono CM.** 2004. Treatment of mice with the neutrophil-depleting antibody RB6-8C5 results in early development of experimental Lyme arthritis via the recruitment of Gr-1- polymorphonuclear leukocyte-like cells. Infect Immun **72:**4956–4965. http://dx.doi.org/10.1128/IAI.72.9.4956-4965.2004.
75. **Xu Q, Seemanapalli SV, Reif KE, Brown CR, Liang FT.** 2007. Increasing the recruitment of neutrophils to the site of infection dramatically attenuates *Borrelia burgdorferi* infectivity. J Immunol **178:**5109–5115. http://dx.doi.org/10.4049/jimmunol.178.8.5109.
76. **Van Rooijen N, Sanders A.** 1994. Liposome mediated depletion of macrophages: mechanism of action, preparation of liposomes and applications. J Immunol Methods **174:**83–93. http://dx.doi.org/10.1016/0022-1759(94)90012-4.
77. **Birge RB, Ucker DS.** 2008. Innate apoptotic immunity: the calming touch of death. Cell Death Differ **15:**1096–1102. http://dx.doi.org/10.1038/cdd.2008.58.
78. **Savill J, Dransfield I, Gregory C, Haslett C.** 2002. A blast from the past: clearance of apoptotic cells regulates immune responses. Nat Rev Immun **2:**965–975. http://dx.doi.org/10.1038/nri957.
79. **Linder S, Heimerl C, Fingerle V, Aepfelbacher M, Wilske B.** 2001. Coiling phagocytosis of *Borrelia burgdorferi* by primary human macrophages is controlled by CDC42Hs and Rac1 and involves recruitment of Wiskott-Aldrich syndrome protein and Arp2/3 complex. Infect Immun **69:**1739–1746. http://dx.doi.org/10.1128/IAI.69.3.1739-1746.2001.
80. **Modolell M, Schaible UE, Rittig M, Simon MM.** 1994. Killing of *Borrelia burgdorferi* by macrophages is dependent on oxygen radicals and nitric oxide and can be enhanced by antibodies to outer surface proteins of the spirochete. Immunol Lett **40:**139–146. http://dx.doi.org/10.1016/0165-2478(94)90185-6.
81. **Kraiczy P, Skerka C, Brade V, Zipfel PF.** 2001. Further characterization of complement regulator-acquiring surface proteins of *Borrelia burgdorferi*. Infect Immun **69:**7800–7809. http://dx.doi.org/10.1128/IAI.69.12.7800-7809.2001.
82. **Radolf JD, Robinson EJ, Bourell KW, Akins DR, Porcella SF, Weigel LM, Jones JD, Norgard MV.** 1995. Characterization of outer membranes isolated from Treponema pallidum, the syphilis spirochete. Infect Immun **63:**4244–4252.
83. **Howe TR, LaQuier FW, Barbour AG.** 1986. Organization of genes encoding two outer membrane proteins of the Lyme disease agent *Borrelia burgdorferi* within a single transcriptional unit. Infect Immun **54:**207–212.
84. **Ohnishi J, Piesman J, de Silva AM.** 2001. Antigenic and genetic heterogeneity of *Borrelia burgdorferi* populations transmitted by ticks. Proc Natl Acad Sci U S A **98:**670–675. http://dx.doi.org/10.1073/pnas.98.2.670.
85. **de Silva AM, Telford SR, III, Brunet LR, Barthold SW, Fikrig E.** 1996. *Borrelia burgdorferi* OspA is an arthropod-specific transmission-blocking Lyme disease vaccine. J Exp Med **183:**271–275. http://dx.doi.org/10.1084/jem.183.1.271.
86. **Moore MW, Cruz AR, LaVake CJ, Marzo AL, Eggers CH, Salazar JC, Radolf JD.** 2007. Phagocytosis of *Borrelia burgdorferi* and *Treponema pallidum* potentiates innate immune activation and induces gamma interferon production. Infect Immun **75:**2046–2062. http://dx.doi.org/10.1128/IAI.01666-06.
87. **Zhao JF, Chen HH, Ojcius DM, Zhao X, Sun D, Ge YM, Zheng LL, Lin X, Li LJ, Yan J.** 2013. Identification of *Leptospira interrogans* phospholipase C as a novel virulence factor responsible for intracellular free calcium ion elevation during macrophage death. PLoS One **8:**e75652. http://dx.doi.org/10.1371/journal.pone.0075652.
88. **Schwende H, Fitzke E, Ambs P, Dieter P.** 1996. Differences in the state of differentiation of THP-1 cells induced by phorbol ester and 1,25-dihydroxyvitamin D3. J Leukoc Biol **59:**555–561.
89. **Yang X, Coleman AS, Anguita J, Pal U.** 2009. A chromosomally encoded virulence factor protects the Lyme disease pathogen against host-adaptive immunity. PLoS Pathog **5:**e1000326. http://dx.doi.org/10.1371/journal.ppat.1000326.
90. **Fischer JR, LeBlanc KT, Leong JM.** 2006. Fibronectin binding protein BBK32 of the Lyme disease spirochete promotes bacterial attachment to glycosaminoglycans. Infect Immun **74:**435–441. http://dx.doi.org/10.1128/IAI.74.1.435-441.2006.
91. **Hawley KL, Olson CM, Jr, Iglesias-Pedraz JM, Navasa N, Cervantes JL, Caimano MJ, Izadi H, Ingalls RR, Pal U, Salazar JC, Radolf JD, Anguita J.** 2012. CD14 cooperates with complement receptor 3 to mediate MyD88-independent phagocytosis of *Borrelia burgdorferi*. Proc Natl Acad Sci U S A **109:**1228–1232. http://dx.doi.org/10.1073/pnas.1112078109.
92. **Montgomery RR, Nathanson MH, Malawista SE.** 1994. Fc- and non-Fc-mediated phagocytosis of *Borrelia burgdorferi* by macrophages. J Infect Dis **170:**890–893. http://dx.doi.org/10.1093/infdis/170.4.890.
93. **Petnicki-Ocwieja T, Chung E, Acosta DI, Ramos LT, Shin OS, Ghosh S, Kobzik L, Li X, Hu LT.** 2013. TRIF mediates Toll-like receptor 2-dependent inflammatory responses to *Borrelia burgdorferi*. Infect Immun **81:**402–410. http://dx.doi.org/10.1128/IAI.00890-12.
94. **Wooten RM, Ma Y, Yoder RA, Brown JP, Weis JH, Zachary JF, Kirschning CJ, Weis JJ.** 2002. Toll-like receptor 2 is required for innate, but not acquired, host defense to *Borrelia burgdorferi*. J Immunol **168:**348–355. http://dx.doi.org/10.4049/jimmunol.168.1.348.